

NRC Publications Archive Archives des publications du CNRC

An experimental study on NO_x emissions of a heavy-duty diesel engine during cold start and idling

Dev, Shouvik; Guo, Hongsheng; Liko, Brian; Lafrance, Simon; Conde, Aaron

This publication could be one of several versions: author's original, accepted manuscript or the publisher's version. / La version de cette publication peut être l'une des suivantes : la version prépublication de l'auteur, la version acceptée du manuscrit ou la version de l'éditeur.

For the publisher's version, please access the DOI link below. / Pour consulter la version de l'éditeur, utilisez le lien DOI ci-dessous.

Publisher's version / Version de l'éditeur:

<https://doi.org/10.4271/2021-01-0535>

SAE Technical Papers, 2021-04-06

NRC Publications Archive Record / Notice des Archives des publications du CNRC :

<https://nrc-publications.canada.ca/eng/view/object/?id=e807262a-ac5d-44a4-ac24-56bd81ca21c2>

<https://publications-cnrc.canada.ca/fra/voir/objet/?id=e807262a-ac5d-44a4-ac24-56bd81ca21c2>

Access and use of this website and the material on it are subject to the Terms and Conditions set forth at

<https://nrc-publications.canada.ca/eng/copyright>

READ THESE TERMS AND CONDITIONS CAREFULLY BEFORE USING THIS WEBSITE.

L'accès à ce site Web et l'utilisation de son contenu sont assujettis aux conditions présentées dans le site

<https://publications-cnrc.canada.ca/fra/droits>

LISEZ CES CONDITIONS ATTENTIVEMENT AVANT D'UTILISER CE SITE WEB.

Questions? Contact the NRC Publications Archive team at

PublicationsArchive-ArchivesPublications@nrc-cnrc.gc.ca. If you wish to email the authors directly, please see the first page of the publication for their contact information.

Vous avez des questions? Nous pouvons vous aider. Pour communiquer directement avec un auteur, consultez la première page de la revue dans laquelle son article a été publié afin de trouver ses coordonnées. Si vous n'arrivez pas à les repérer, communiquez avec nous à PublicationsArchive-ArchivesPublications@nrc-cnrc.gc.ca.

An Experimental Study on NO_x Emissions of a Heavy-Duty Diesel Engine during Cold Start and Idling

Author, co-author (Do NOT enter this information. It will be pulled from participant tab in MyTechZone)

Affiliation (Do NOT enter this information. It will be pulled from participant tab in MyTechZone)

Abstract

In North America, heavy-duty diesel engines for on-road use have to meet strict regulations for their emissions of nitric oxide and nitrogen dioxide (cumulatively referred to as 'NO_x') besides other criteria pollutants. Over the next decade, regulations for NO_x emissions are expected to become more stringent in North America. One of the major technical barriers for achieving in-use NO_x emissions commensurate with the levels determined from in-laboratory test procedures required by regulations is controlling NO_x emissions during cold start and engine idling. Since the exhaust gas temperature can be low during these conditions, the effectiveness of the exhaust after-treatment (EAT) system may be reduced. Under colder climate conditions like in Canada, the impact may be even more significant. In the experimental study of this paper, certain engine operation parameters such as the fuel injection timing, fuel injection frequency per cycle, engine speed, and exhaust gas recirculation (EGR) ratio are evaluated for their impact on NO_x emissions during idling conditions. The study is conducted on a single-cylinder, four stroke, heavy-duty research engine equipped with an intake charge cooling system and an EAT system with independent control of diesel exhaust fluid injection. In order to partially simulate a cold operational environment for the engine and highlight the associated challenges for NO_x control, tests are conducted at an intake charge temperature of 10 degrees Celsius below the Federal Test Protocol mandated cold start temperature, and auxiliary cooling is used for the engine oil and coolant to maintain the temperature of these fluids to below 50 degrees Celsius. Results indicate that in-use NO_x emissions can be more than an order of magnitude higher than levels determined by the present in-laboratory test procedures required by regulations immediately after cold start and during engine idling. Using a combination of medium levels of EGR, elevated idling speed and injection timing control, the gas temperature in the exhaust manifold can be ramped up to higher than 200 °C in a short duration while simultaneously reducing engine-out NO_x emissions. The use of a fuel post-injection during the expansion stroke can further reduce NO_x emissions at the expense of thermal efficiency.

Introduction

Nitrogen oxides (NO_x) made up of nitric oxide (NO) and nitrogen dioxide (NO₂) are one of the six key air pollutants which can cause harmful effects to the environment and human health [1]. In 2018, on-road heavy-duty vehicles (HDVs) accounted for approximately 14% of Canada's NO_x emissions [2]. The current Canadian NO_x emission standards for engines of on-road heavy-duty vehicles is 0.2 g/bhp-hr in

alignment with the standards of the United States (US) Environment Protection Agency (EPA). In November 2018, EPA launched the Cleaner Trucks Initiative (CTI) with the intention to update the current NO_x emission regulations [3]. In January 2020, EPA released an Advance Notice of Proposed Rule (ANPR) to further describe its plans for overhauling the emission standards for HDVs [4]. This ANPR described EPA's intentions of lowering NO_x emission standards, improving test procedures and test cycles to provide real world emission reductions, updating certification and in-use testing protocols, and mandating longer useful life of emission control components, among others [4]. Though the ANPR does not explicitly specify any particular values, ultra-low NO_x emission standards (up to 90% reduction from current 0.2 g/bhp-hr) are under consideration [5]. In response to the CTI, the Manufacturers of Emissions Controls Association (MECA) released a report on technology feasibility for HDVs to achieve this 90% reduction in NO_x emissions by 2027 [6]. MECA expressed confidence that commercially available engine technologies and advanced exhaust after-treatment (EAT) system designs can achieve the NO_x reduction target at a nominal increment to vehicle cost. HDV operation in Canada is subject to unique conditions. HDVs tend to operate in a cold climate for extended periods, and can have lengthy periods of engine idling due to cabin heating requirements and long border wait times [7]. Future ultra-low NO_x HDV technology development must consider these unique conditions for the technologies to be successful in reducing real-world NO_x emissions from HDVs in Canada and other cold climates.

NO_x emissions during the cold start period and idling can be an impediment to achieving ultra-low NO_x emissions in real-world driving and over emission certification cycles [8]. NO_x emissions from HDVs may be reduced to ultra-low levels through optimization of the in-cylinder processes and implementation of sophisticated EAT systems. During cold start, especially in Canadian winters, the EAT system may take a significant amount of time to reach operating temperatures. Extended engine idling can prevent fast warm-up of the EAT as well. The EAT system consists of various components such as diesel oxidation catalyst (DOC), diesel particulate filter (DPF), selective catalytic reduction (SCR) unit, and ammonia slip catalyst (ASC). Upstream of the SCR, urea solution (termed as diesel exhaust fluid or DEF) is injected which then thermally decomposes into ammonia. This ammonia reduces NO_x into nitrogen and oxygen in the SCR unit.

The temperature of the SCR is a critical factor for effective NO_x reduction, and it is important to understand the typical catalyst temperatures that may be encountered during the Federal Test Protocol

FTP) cycle for a heavy-duty engine. It may take more than 600 seconds after the initial start-up, for the SCR inlet temperature to reach 200 °C [9]. Below 200 °C, the NO_x conversion efficiency of the SCR is usually less than 50%. Therefore, a large portion of the engine-out NO_x emissions can exit the tail-pipe untreated. Iron-zeolite (Fe-Z) and copper-zeolite (Cu-Z) catalysts typically used in SCR units tend to have different NO_x conversion rates at different SCR-inlet temperatures and NO₂/NO_x [10]. Increasing NO₂/NO_x ratio increases the NO_x conversion rate. When NO₂/NO_x ratio is zero, Cu-Z catalysts have higher NO_x conversion rates over Fe-Z catalysts. The trend is reversed at the lowest temperatures when NO₂/NO_x ratio is 0.5.

In modern diesel engines, minimizing the in-cylinder NO_x production involves optimizing the in-cylinder temperature and oxygen concentration besides other operating parameters. One of the most common in-cylinder methods of NO_x control is the use of exhaust gas recirculation (EGR). In engines with EGR, a portion of the exhaust gas is directed back into the engine intake [11]. Use of EGR is an established method to reduce the in-cylinder NO_x formation in diesel-fueled CI engines [11-12]. The reduction of NO_x emissions by the application of EGR is caused by factors such as decrease in the intake oxygen concentration (dilution effect), increase in the specific heat of the cylinder charge (thermal effect), and endothermic dissociation of species such as water and CO₂ (chemical effect) [13]. One disadvantage of EGR is that it may cause an increase in the soot emissions. This is typically referred to as the NO_x-soot trade-off. It may also increase the hydrocarbon emissions under certain conditions due to lower temperatures and increased ignition delay.

In addition to controlling engine-out NO_x, the exhaust thermal management is necessary for the EAT system to be functioning at high efficiency. Cold temperatures may make this particularly difficult. Sakunthalai et al. studied the impact of cold ambient conditions on the cold start and idle emissions of a light duty diesel engine [14]. Tests were performed in a climate controlled engine dynamometer test facility with temperatures ranging from -20 to 20 °C. The engine speed was rapidly increased and then the engine was allowed to coast down to idling speed. At lower ambient temperatures, it took more cranking cycles to start the engine, and longer periods to reach target engine speed and eventually settle down into the idling speed. This was due to increased misfire cycles at low temperatures. The adverse impact of colder ambient temperatures on the NO_x emissions was significant since the EGR calibration on the test engine would cause the EGR valve to open only when the manifold temperature was equal or higher than the ambient temperature to prevent condensation in the EGR lines. At cold temperatures, the friction and pumping losses were also higher which increased the effective load on the engine.

Bai et al. investigated thermal management strategies on the NO_x emissions of a heavy-duty diesel engine with an EAT system [15]. The NO_x conversion efficiency decreased and the ammonia slip increased with decreasing exhaust temperature. The authors demonstrated the use of intake throttling to increase the exhaust temperature during cold start conditions at the expense of marginal decrease in the fuel economy. A large scale study of real-world exhaust temperature and NO_x conversion efficiency was conducted by Boriboonsomsin et al. for 90 diesel fueled HDVs which met the 2010 NO_x emission standard using SCR systems [16]. The HDVs were deployed in various vocations in the state of California, USA. The vehicles in the study spent 11-70% of their operation time with SCR temperatures below 200 °C which meant that the SCR conversion efficiencies were minimized. Moreover, copper-zeolite (Cu-zeolite) SCR systems were found to have better low temperature performance than iron-zeolite (Fe-

zeolite) SCR systems. In general, the optimum operational temperature for Cu-zeolite SCR systems was 225-350 °C.

South West Research Institute (SwRI), with the support of California Air Resources Board, has pioneered experimental research on heavy-duty ultra-low NO_x emissions [8, 17-18] and shared results on their modified cold calibration strategy [19]. Using this strategy, they were able to reduce the time required to reach their target DOC outlet temperature by almost 70% compared to the baseline. The cumulative engine-out NO_x was decreased by 68% though the CO₂ emission increased by almost 4% over the Federal Test Protocol Cycle. SwRI also evaluated a number of EAT system configurations which, together with the modified cold calibration strategy of the engine, can meet their 0.02 g/bhp-hr target [20]. This configuration consisted of an active close-coupled selective catalytic reduction (ccSCR) system to treat NO_x during low temperature operation such as cold start and idling periods.

The aim of this research is to build on the existing research by examining NO_x emissions and developing NO_x control strategies during cold start and idling operation relevant to cold climates. Specifically, the effects of engine load, engine speed, EGR quantity, and use of multiple diesel injection events are investigated. In-use tests are conducted on a Class-8 semi-trailer truck compliant with current emission standards. The data is used to identify specific NO_x control challenges associated with winter operation. Thereafter, laboratory tests are conducted under cold intake air conditions with more detailed analysis of specific engine operation parameters on NO_x emissions and exhaust gas temperature. This paper is organized as follows. Immediately succeeding this introduction section is the description of the experimental setup, followed by the methodology, and discussion on the results for the on-road and laboratory testing. This is followed by conclusion and references.

Experimental Setup and Methods

Experimental Setup

In-use Testing

In-use emissions measurements were taken on a Class-8 semi-trailer truck using commercially available Portable Emissions Measurement Systems (PEMS) developed by Sensors Inc. Test vehicle specifications are shown in Table 1. The only modification to the test vehicle was the installation of the PEMS probe and flow meter (Figure 1). The PEMS used a combination of technologies to measure the concentration of CO₂, CO, NO, NO₂, O₂, and Total Hydrocarbons (THC) in the raw tailpipe exhaust gas. The systems were calibrated with NIST-certified gases prior to, and immediately after an in-use test cycle was completed. A mass flow meter, provided with the PEMS, was attached to the exhaust system to determine exhaust flow rate. Leak checks, calibration of the system, and emissions calculations were followed according to 40 CFR 1065 equipment standards. Emissions measurements and ECU data were logged at the beginning of each test event and throughout the duration of the test, capturing the cold start period. ECU data was collected by connecting to the vehicle network using a third-party data logger (DiagRa D, HEM) and via hardware integrated with the PEMS unit. Testing was conducted under a variety of load-speed conditions. These tests were intended to capture the performance of the vehicle under real-world scenarios.

Table 1. Test vehicle specifications

Engine Displacement [L]	12.9
Transmission	16 Speed Fully Automated
Advertised power [kw]	339
Torque [Nm]	2237@900 rpm
Emission Controls	Meets US EPA 2010 standards
Certification	HDV Class 8
Curb Weight [kg/(lbs)]	8,243 (18,173)
Ballast Weight [kg/(lbs)]	18,593 (40,990)
Trailer Weight [kg/(lbs)]	6,019 (13,270)
Test Weight [kg/(lbs)]	32,855 (72,433)

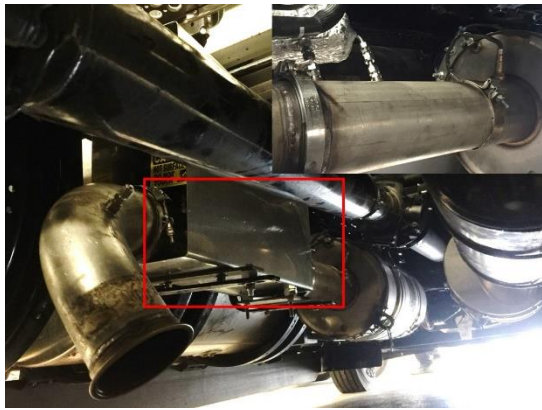


Figure 1. In-use emission measurement – location of PEMS attachments and close-up of sampling ports (inset) downstream of catalysis

Laboratory Testing

The tests were conducted on a Caterpillar 3401 based research engine. This single-cylinder, four-stroke, heavy-duty diesel engine was rated to 74.6 kW and coupled to an eddy-current dynamometer. The engine was modified and instrumented for research. The test setup is shown in Figure 2. The specifications of the engine are listed in Table 2. The stock diesel fuel injection system was replaced by a customized and independently controlled common rail fuel injection system designed for research purpose. This system used a Ganser CRS AG solenoid fuel injector. The fuel rail pressure, diesel injection timing, and pulse width were controlled by National Instruments (NI) hardware (PXI-1031 chassis with PXI-8184 embedded controller and 7813R RIO card connected to a cRIO-9151 expansion chassis) and LabVIEW-based software (Stand-alone Direct Injector Drive System, Drivven Inc.). A Bronkhorst mass flowmeter was used to measure the diesel flow rate. The specifications of the Canadian ultra-low sulphur diesel (ULSD) fuel used in this research are given in Table 3.

Table 2. Test engine specifications

Base Engine Model	Caterpillar 3401 (3400 series)
Number of Cylinders	1
Bore X Stroke	137.2 mm X 165.1 mm
Displacement	2.44 liters
Compression Ratio	16.25:1
Number of Valves	4 (2 – Intake, 2 – Exhaust)
Fuel Delivery - Diesel	Common Rail Direct Injection Ganser CRS AG Injector
Maximum Power Output (stock)	74.6 kW (@2100 rpm)

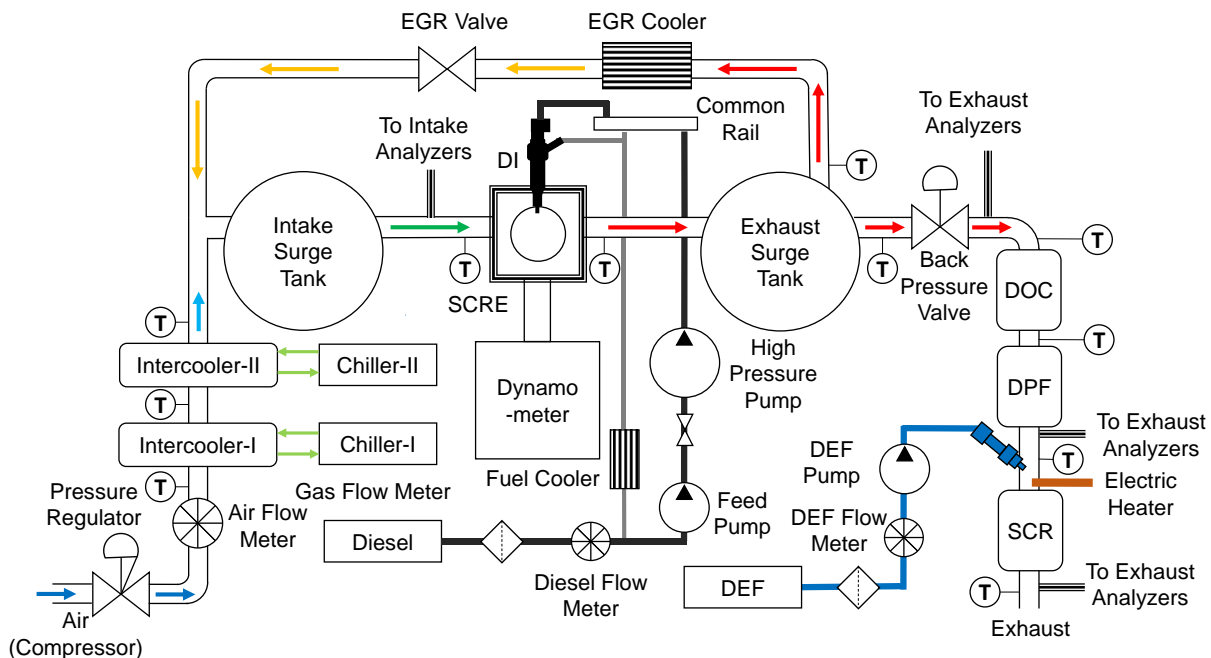


Figure 2. Laboratory test setup

Table 3. Properties of ultra-low sulphur diesel used in laboratory test

Density [kg/m ³]	Cetane number	LHV [MJ/kg]	H/C ratio
814.8	44	44.64	1.90

The test setup also consisted of a conditioned air supply system with independent control of intake charge pressure and temperature. Intake and exhaust surge tanks in the intake and exhaust sides reduced pressure pulsations in the system. A thermal wire type mass flowmeter was used to measure the intake air flow rate (manufactured by Sierra Instruments Inc.). The EGR supply loop consisted of an exhaust back pressure control valve, water-cooled EGR cooling system, and EGR flow control valve. The EGR cooling system consisted of a series of plate heat exchangers. The EGR gas temperature was controlled by modulating the water flow rate into the EGR cooler. This cooled EGR system can be used for preheating and/or decreasing the oxygen concentration of the intake charge by diverting a portion of the exhaust gas into the intake.

Combustion conditions relevant to cold-start at cold weather conditions were simulated by conducting the testing with cooled intake air supply. Given the limitations of the test setup, the target was a stable intake manifold air supply temperature of at least 10 °C below the FTP cold start temperature of 20 °C. The test facility modification included the installation of two high efficiency air to liquid intercoolers in series in the fresh air intake line of the engine (Figure 2). These automotive grade intercoolers were made of aluminum. Each of the intercoolers was connected to a 1.5 kW laboratory chiller circulating a chilled 50:50 mixture of ethylene glycol and water through the intercooler. The chiller temperatures were set to -10 °C. The compressed air supply for the engine was pressure-regulated in multiple stages to provide a stable and controllable air flow into the intercoolers. Thermocouples were installed before and after the intercoolers to monitor the cooling efficiency. The chilled air supply line was insulated to minimize heat absorption from the ambient air. The target intake temperature of 10 °C or below was measured in the intake manifold just upstream of the intake valve.

The engine was also outfitted with coolant and lubricating oil temperature conditioning systems. The test facility is equipped with a cooling tower using water as the working fluid, to cool the lubrication oil and the coolant through a series of heat exchangers. The oil and the coolant temperatures can either be maintained at ~40-50 °C during the test using the cooling water, or allowed to rise gradually after starting the test through the heat dissipation from the in-cylinder combustion. The former provides the ability to simulate the extended period of warm-up required for the engine fluids to reach operational temperature in cold weather. Such a system also ensures that the cooled intake air supply does not heat up drastically when it comes in contact with the intake manifold and the cylinder head. The steady state operating temperature of the oil and coolant for this test setup is 88 °C.

The cylinder pressure was determined by a Kistler 6041A pressure transducer which was flush mounted on the cylinder head. The pressure data was stored at a resolution of 0.2 CAD for 100 consecutive engine cycles using AVL IndiModule combustion analysis system. AVL Digalog Testmate system was used to interface with the engine electronic control unit (ECU) to control the engine load and speed. The exhaust and intake gases of the engine were sampled and analyzed by California Analytical Instruments (CAI) 600 series gas analyzers. The cylinder pressure was determined by a Kistler 6041A pressure transducer which was flush mounted on the cylinder head. The pressure data was stored at a resolution of 0.2 CAD for 100 consecutive engine cycles using AVL IndiModule combustion analysis system. AVL Digalog Testmate system was used to interface with the engine electronic control unit (ECU) to control the engine load and speed. The exhaust and intake gases of the engine were sampled and analyzed by California Analytical Instruments (CAI) 600 series gas analyzers.

exhaust gases analyzed included CO₂, CO, THC, O₂ and NO_x. The intake CO₂ was measured to determine the CO₂-based EGR ratio. The exhaust soot was measured using an AVL 415S smoke meter. The basic configuration of the EAT system consisted of a DOC and DPF assembled in one canister, and a urea-based selective catalytic reduction (SCR) system using copper zeolite as the catalyst. The EAT system was installed downstream of the exhaust surge tank and the exhaust throttle valve. The exhaust temperature was measured in the exhaust manifold located just downstream of the exhaust valve. A pressure transducer was also installed upstream of the DPF to monitor DPF soot loading. Additionally, temperature and gas sampling probes were installed at multiple locations in the exhaust line for monitoring and data collection. Emissions were measured at the engine and the tail-pipe outlets. This paper will focus on the engine-out NO_x emissions.

Experimental Methods

Certain terms must be defined at the outset for enabling interpretation of the test results. The cylinder pressure signal was used as the primary input for the conventional net heat release analysis (HRR) using Equation (1). The unit of net heat release rate was joule per crank angle degree [J/CAD]. The brake thermal efficiency (BTE) was calculated using Equation (2) and expressed as a percentage.

$$HRR_{net} = \frac{1}{\gamma - 1} \left[\gamma p \frac{dV}{d\theta} + V \frac{dp}{d\theta} \right] \quad (1)$$

$$BTE = 100 \times \frac{3600 \times Power_{brake}}{LHV_f \times m_f} \quad (2)$$

where γ was the ratio of specific heat at constant pressure to that at constant volume (calculated as a function of in-cylinder gas composition and temperature), p was the measured cylinder pressure [Pa], V was the cylinder volume [m³], θ was the crank angle in degrees [CAD], $Power_{brake}$ was the measured brake power of the engine from the dynamometer [kW], LHV_f was the lower heating value of the fuel [kJ/g], and m_f was the mass flow rate of the fuel [g/hour].

One engine cycle was expressed as -360 to 360 CAD, with all crank-based timings expressed as CAD after top dead center (ATDC). The compression TDC was 0 CAD ATDC. Specific combustion timing metrics were calculated from the heat release analysis. ‘CA50’ corresponded to the combustion phasing and was defined as the crank angle at which 50% of the cumulative heat release occurred [CAD ATDC]. Crank angles corresponding to 10% and 90% of the total heat release were denoted by ‘CA10’ and ‘CA90’, respectively [CAD ATDC]. The combustion duration was defined as the time difference between CA90 and CA10 and expressed in [CAD]. The volumetric EGR ratio (expressed as a percentage) which quantified the amount of EGR used was calculated through the relation –

$$EGR_{CO_2} = 100 \times \frac{CO_{2\ inlet} - CO_{2\ ambient}}{CO_{2\ exhaust}} \quad (3)$$

where $CO_{2\ inlet}$, $CO_{2\ exhaust}$, and $CO_{2\ ambient}$, were the volume fractions of carbon dioxide at the engine inlet after mixing of EGR, engine exhaust, and engine inlet before mixing of EGR respectively. Engine load was given by the brake mean effective pressure (BMEP) which was calculated using the following relation with the unit [bar] –

$$BMEP = \frac{4\pi}{10^5} \times \frac{T}{V_d} \quad (4)$$

where T is the brake torque of the engine determined using the dynamometer [Nm] and V_d is the displacement volume of the engine [m³].

Before starting the test, the engine and EAT system were preconditioned by motoring the engine with an electric motor at 650 rpm while cold air was circulated through the system. The chillers circulated the glycol-water solution through the intercooler with the EGR valve closed and the back pressure valve fully open. This caused the fresh air intake temperature to decrease. The post-intercooler air temperature was in the range of -4 ± 2 °C. During this cooling down period, the air flow rate was maintained at 100 kilograms per hour (kg/h). Though efforts were made to insulate the intake plumbing of the engine, the thermal mass of the intake line was significant and the test cell ambient temperature could only be maintained in a limited range of 20 ± 2 °C. Therefore, the lowest stable gas temperature at the intake manifold that could be achieved with the oil and coolant at their target temperatures was 10 °C. Once the target gas temperature was achieved in the intake and exhaust manifolds, the intake pressure was set to 0.09 megapascal (MPa).

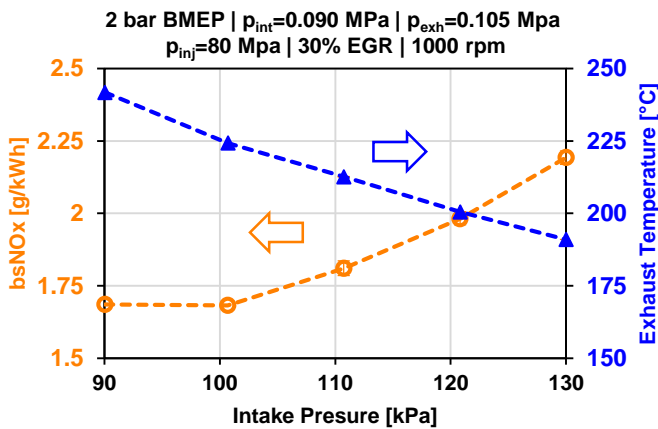


Figure 3. Effect of intake pressure on brake specific NOx emissions and exhaust temperature

The purpose of the research was to develop an understanding of operational parameters that can enable fast temperature increase of the exhaust gas and reduce NOx emissions. Exploratory testing showed that increasing the intake pressure caused the NOx emissions to increase and the exhaust temperature to decrease (example shown in Figure 3). The increase in NOx emissions was due to the increase in the in-cylinder air-fuel ratio (relative air-fuel ratio increased from 2.27 to 3.41 in the given example as intake pressure was increased) and the increase in the in-cylinder pressure before injection. Fuel droplets had improved access to oxygen and NOx formation rate was enhanced [21-23]. Exhaust temperature decreased as the mass air flow through the engine increased causing greater amount of energy to be dissipated through the system. Field testing done on heavy-duty trucks had shown that after a cold start, as the engine settled into idle, typically there was negligible intake boost (discussed later). Taking all these factors into consideration and the benefit of throttling the intake flow [15], the intake pressure was set to slightly below atmospheric pressure at 0.09 MPa. Lower values were not considered for two reasons – ensure that the relative air fuel ratio at all test conditions including steady state testing was not below 1.8 (minimize soot formation), and avoid

significant decrease in the volumetric efficiency of the engine. The exhaust back pressure was set at 0.015 MPa over the intake pressure to drive the EGR gas into the intake. This was the lowest pressure differential which allowed the maximum EGR ratios to be achieved with the EGR valve fully open. Hence, the exhaust pressure was 0.105 MPa.

Diesel injection rail pressure was set to 80 MPa. Injection pressures can vary between 30 to 250 MPa for modern diesel engines. This was the lowest injection pressure based on the injector map, which was suitable for all test conditions including steady state idling tests with multiple injections. In order to initiate the cold start test, fuel injection was enabled and the electric motor was decoupled from the engine. Three engine idle speeds were investigated – 650, 1000, and 1350 rpm. For the lowest engine speed of 650 rpm, the fueling was first set to no load idle and as soon as the engine reached 650 rpm no load idle, the load was ramped up from 0-2 bar BMEP. 2 bar BMEP was the lowest load at which the exhaust manifold gas temperature of at least 200 °C could be achieved for all test conditions. This corresponded to approximately 12.5% load for this test engine. The engine was allowed to subsequently reach stable speed at this load (± 5 rpm). For the 1000 and 1350 rpm cases, the same sequence of actions was undertaken with one exception – the engine speed was set to the desired value before the load was applied. These steady state idling tests involved studying the effects of two engine parameters – EGR ratio and post-injection timing. The experimental conditions are listed in Table 4.

Table 4. Experimental conditions for laboratory testing

Parameter	Effect of EGR Ratio	Effect of Post Injection Timing
Load in BMEP [bar]	2	2
EGR Ratio [%]	0/5/10/15/20/25/30	30
Data Collection Period [s]	180s	180s
Number of Diesel Injections [-]	1	2
Main Diesel Injection Timing [CAD ATDC]	-1/-7/-12	-4.5/-9.5/-14
Post Injection Timing [CAD ATDC]	Not applicable	10/15/20/25/30
Post Injection Ratio (Main:Post)	Not Applicable	60 :40
Engine Speed (N) [rpm]	650/1000/1350	
Initial Intake Temperature (T_{in}) [°C]	10 \pm 1	
Intake Pressure (p_{in}) [MPa absolute]	0.09	
Exhaust Pressure (p_{exh}) [MPa absolute]	0.105	
Diesel Injection Pressure (p_{inj}) [MPa]	80	
EGR Gas Temperature (after EGR valve) [°C]	~30 \pm 2	
Coolant Temperature [°C]	40 \pm 2	
Lubricating Oil Temperature [°C]	50 \pm 2	

The coolant and lubricating oil temperatures were 40 and 50 °C respectively. EGR outlet gas temperature was maintained at ~30 °C. The diesel injection (DI) timing was set for a CA50 of 9 \pm 1 CAD ATDC for each engine speed case. Based on the past experience with this engine test setup, this CA50 range is typically associated with maximum thermal efficiency. The EGR ratio was gradually increased to perform the EGR ratio sweep. For each EGR ratio, the engine was deemed to be in stable condition when the exhaust temperature change was within ± 1 °C and the NOx emissions were ± 5 ppm. These values were within the error range of the measurement equipment. The data

was collected at a resolution of 1 Hz over a 180 second period, and the average value and standard deviation were reported as the result. Further NO_x reduction and exhaust gas temperature increase was investigated by enabling a second post-injection at 30% EGR with a post injection (PI) timing of 10 CAD ATDC. The main DI timing was advanced at this point to adjust the CA50 to 9±1 CAD ATDC again. The post-injection (PI) timing was gradually retarded to perform the PI timing sweep with the main DI timing constant. These steps were repeated for each engine speed.

Results and Discussion

This section is divided into three sub-sections. The results of in-use testing are shown in the first sub-section. The results of laboratory testing with increasing EGR, and effect of the post-injection timing are presented in the second and third sub-sections, respectively.

In-use Testing Results

In-use testing for three different load-speed data-points (denoted by 'DP' followed by the number) will be discussed to highlight some specific in-use challenges associated with cold weather operation. Test durations were typically an hour but in relation to the present discussion on cold start and idling, the focus will be on the initial period of the test cycle. The throttle input, engine load, engine speed, and ground speed readings are shown in Figure 4 for the first 500 seconds. The corresponding ambient, intake and exhaust manifold temperatures together with the exhaust flow rate are shown in Figure 5. The idling speed for this powertrain is 650 rpm and the time scale starts at the instant the engine reaches this set point after firing.

DP-1 is related to idling at low load (~15-20%) for majority of the 500 second period and subsequent shut-down except instances of throttle input at the start and between the 100-200 second period. The former causes corresponding changes in the engine load and speed. The latter causes increase in the load with slight change in engine speed and short duration movement of the vehicle (creep forward for 5 seconds). Otherwise, the vehicle remains stationary during the testing period. DP-2 and DP-3 represent urban driving situations in which the vehicle accelerates and decelerates with occasional stops. Both DP-2 and DP-3 have warm-up period during which the vehicle remains stationary with the engine at idle speed. For all these three conditions, the ambient temperatures are in the range of -16 to -13 °C and remain constant during the initial 500 second period of the test cycle (Figure 5).

For DP-1 and DP-3, the vehicle is soaked overnight indoors at a temperature of ~23 °C. For DP-2, the vehicle is parked outdoors overnight. Hence, the intake (manifold) gas temperatures are higher for DP-1 and DP-3 since the lubricating oil and the coolant are also at a higher initial temperature (not shown). Moreover, the idling load is higher for DP-2 probably due to the need for faster engine warm-up. Since the intake air flow rate changes with change in engine speed and load, the intake temperature fluctuates. The engine load and speed are generally higher for DP-2 in comparison to DP-3 in keeping with getting to higher ground speed faster, therefore the intake temperature starts increasing earlier as the engine warms up (Figure 4 and Figure 5).

Exhaust temperature (shown in Figure 5) is measured immediately downstream of the SCR and upstream of the exhaust gas sampling location. During warm-up, the exhaust gas temperature is expected to decrease across the SCR due to heat loss, therefore the SCR outlet gas temperature would be lower than the inlet gas temperature which

typically determines the start of DEF injection. By analyzing the post-SCR exhaust gas temperature, engine load, and the instantaneous tail-pipe NO_x, it is possible to determine if the SCR is operational. For DP-1, since the vehicle is mostly idling, the exhaust temperature remains constant at ~50 °C. Exhaust temperature of DP-3 (~72 °C) is initially higher than that of DP-1 since the engine load is marginally lower which causes the exhaust mass flow rate to be lower as well (Figure 5 – first 150 seconds). For DP-2, the exhaust gas temperature initially decreases as the idling load decreases marginally, and eventually the exhaust gas temperature starts increasing as the engine speed and load are increased when the vehicle is in motion. For all the three test points, the exhaust temperature is lower than 100 °C for at least the first 400 seconds of the test, which is insufficient for catalytic reduction of NO_x in the SCR.

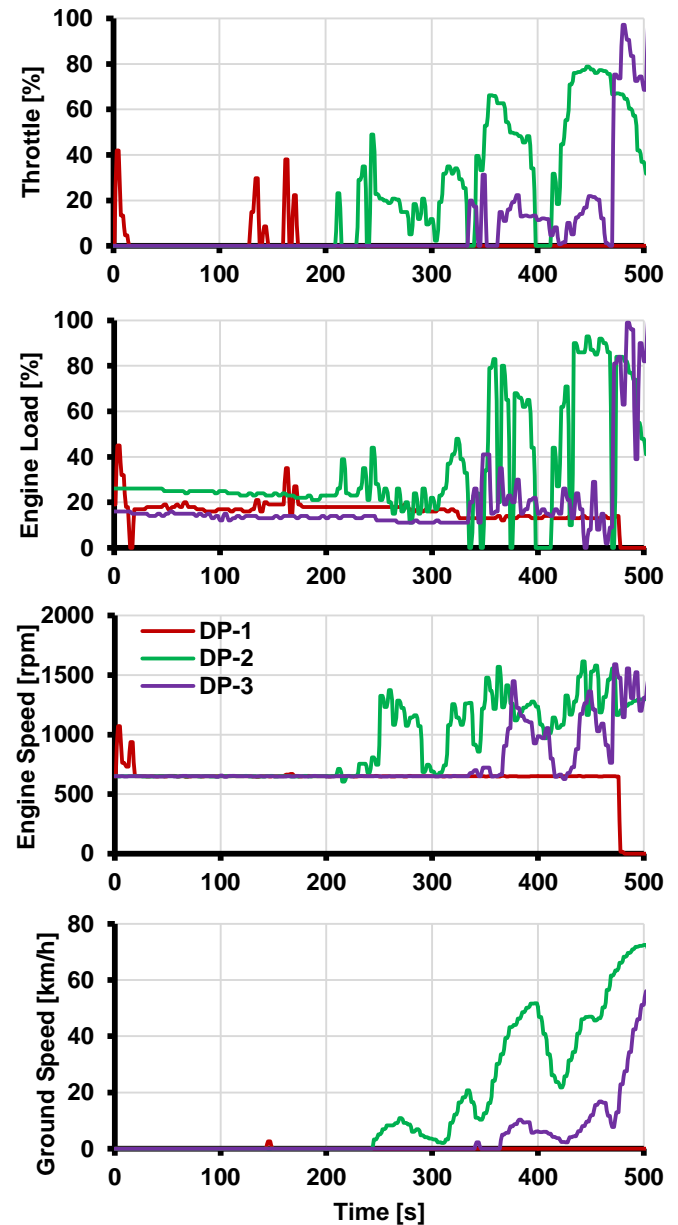


Figure 4. (From top) Throttle position, engine load, engine speed and ground speed of in-use test.

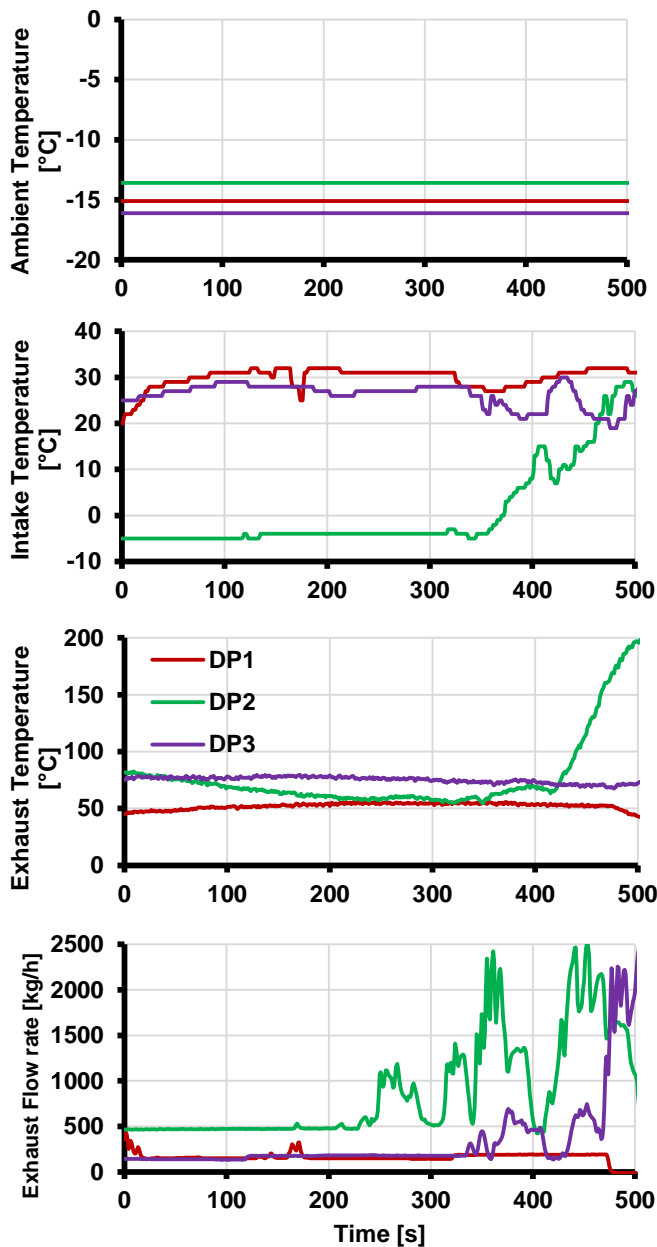


Figure 5. (From top) Ambient temperature, intake temperature, exhaust temperature and exhaust flow rate of in-use test.

Figure 6 shows the tail-pipe NOx emissions for the test data points and the intake manifold pressure. The NOx emissions and manifold pressure of DP-2 correlate with the engine load. During idling, the turbocharger is inactive since the intake manifold pressure is ~0 kPa gauge. DP-2 also has the highest instantaneous NOx emission rates during idling over the first 400 seconds while those of DP-3 and DP-1 are low. This is due to the higher engine load during idling for DP-2 to overcome the low intake temperature. A higher load leads to increased intake pressure and fuel input which causes subsequently greater combustion temperatures. During the 400-500 second period, there is another spike in load but the instantaneous NOx emissions for DP-2 are reduced. This is probably due to the initiation of NOx reduction in the SCR since the exhaust temperature is increasing during this period (Figure 5). For DP-1 and DP-3, the NOx emissions are generally low since there is limited NOx production probably due to the low peak in-

cylinder temperatures at fuel lean conditions associated with low engine load and speed. However, owing to the low exhaust temperatures, it can be expected that the SCR is mostly inactive throughout the first 500 seconds for these cases, and the tail-pipe NOx is equivalent to the engine-out NOx. The estimated brake specific NOx emissions for DP-1, DP-2 and DP-3 averaged over the 500 second period are 0.66 (0.49), 2.87 (2.14) and 1.61 (1.2) g/kWh (values in parentheses are in g/bhp-hr) respectively, which are all significantly higher than the current standard. These are estimates calculated using the engine torque and speed reported by the ECU. It is expected that over a longer driving cycle, as the SCR temperature stabilizes and the engine warms up, the average NOx emissions will be lower. However, achieving future ultra-low NOx emissions in real driving conditions or during extended idling periods will require efforts to minimize engine-out NOx while rapidly increasing the exhaust gas temperature.

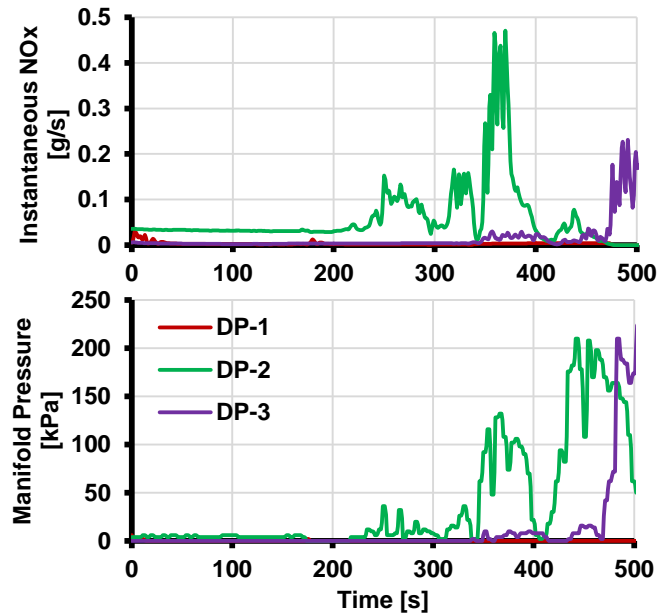


Figure 6. Instantaneous NOx (top) and manifold pressure (bottom) of in-use test.

Laboratory Test – Effect of EGR

In this section, the results for steady state idling tests are presented at a load of 2 bar BMEP. The purpose is to highlight the effect of EGR at different engine speeds. In order to partially simulate a cold operational environment for the engine and highlight the associated challenges for NOx control, tests are conducted at an intake charge temperature of 10 °C, and auxiliary cooling is used for the engine oil and coolant to maintain their temperatures at 50 °C and 40 °C, respectively. The EGR temperature is also maintained at 30 °C though typically the EGR cooler is by-passed during cold start and warm-up in vehicles. The injection timing is fixed during the EGR sweep and denoted by the Start of Diesel Injection (SODI) in the figures. Figure 7 shows the cylinder pressure and heat release rate traces for the three engine speeds of 650 (low), 1000 (medium), and 1350 (high) rpm without and with EGR. The effect of EGR in reducing the intensity of combustion is apparent. The peak cylinder pressure decreases, and the crank position of the peak heat release rate retards with the introduction of EGR. The peak magnitude of the heat release rate is decreased as well. The peak magnitude of the heat release rate increases with the decrease in the engine speed [24-25]. As the engine speed decreases, the temporal duration of each engine cycle increases, which provides

a longer ignition delay period for the diesel to mix with the air in the cylinder before ignition. As a result, more diesel is premixed with air before ignition, which causes a larger peak heat release rate, followed by a smaller peak heat release rate due to diffusion type of combustion at a lower engine speed. It can be seen in Figure 7 that the diffusion peak tends to get less prominent as the engine speed decreases. The injection timing for each engine speed was based on setting the initial CA50 at 9 ± 1 CAD ATDC except for the low speed case (for reasons discussed later).

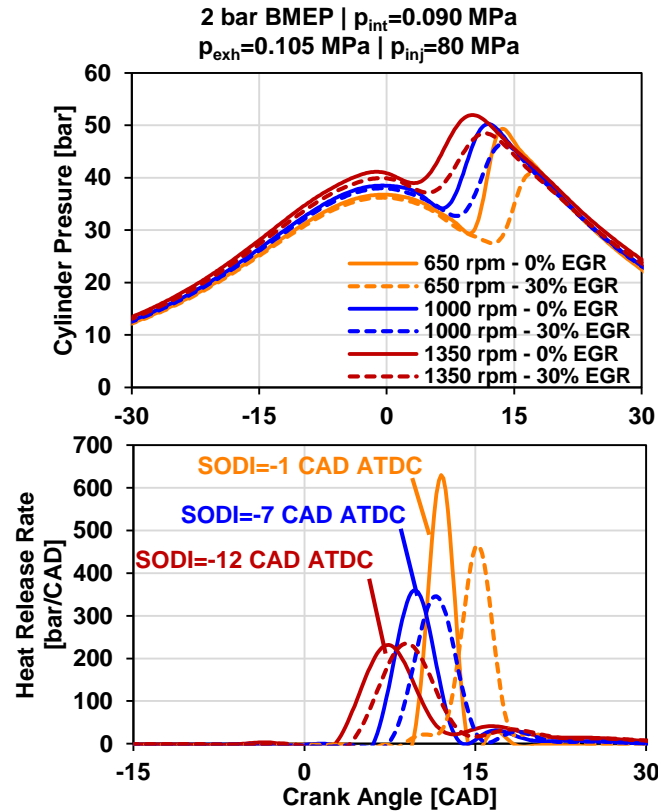


Figure 7. Effect of EGR rate on the cylinder pressure (top) and heat release rate (bottom)

The following figures show the variation of each steady state parameter at a particular engine speed as the EGR ratio is increased. One of the main objectives of this research is to test intake temperature conditions relevant to colder climates. The air flow rate and the intake temperature are shown in Figure 8. The air flow rate increases with increasing engine speed since the engine has more intake strokes per unit time. Use of EGR replaces a part of the fresh air charge into the engine by the exhaust gas, and therefore the fresh air flow rate decreases. Since the tests are started after the coolant and lubricating oil were at steady temperatures of 40 and 50 °C, respectively, the intake temperature drifted slightly upward from the target value of 10°C. The EGR temperature is maintained at 30 °C but it still causes the intake temperature to increase by almost 8 degrees over the EGR sweep since the quantity of exhaust gas mixing with the fresh air intake increases. While EGR is typically used to reduce the in-cylinder NOx formation, for cold operating conditions, it has the added benefit of increasing the intake temperature which in turn can aid in exhaust thermal management. A consequence of increasing EGR is the reduction in the overall relative air-fuel ratio (λ) which decreases from ~ 3.1 - 3.4 at 0% EGR to 2.1 - 2.3 at 30% EGR (not shown). The engine

load remains constant though the fresh air flow rate decreases. This causes the overall air-fuel ratio in the engine to become lower.

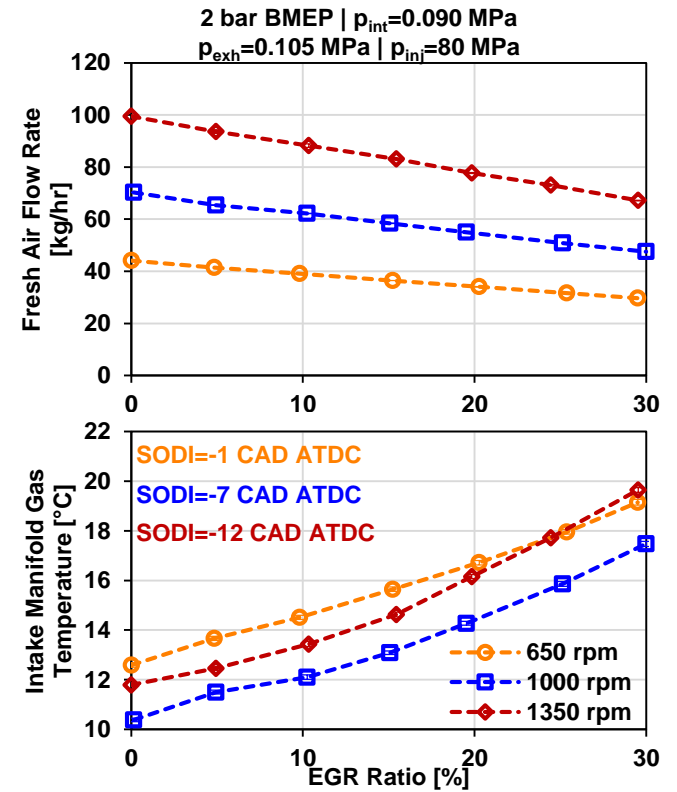


Figure 8. Intake fresh air flow rate (top) and manifold gas temperature (bottom) change with EGR

The combustion phasing, denoted by CA50, is an important metric for relating efficiency and NOx formation. If the CA50 is too early, the released fuel energy may work against the engine compression. If the CA50 is too late, the fuel combustion may be incomplete. In both scenarios, the BTE is expected to decrease. Retarding the CA50 tends to decrease NOx emissions since it causes thermal NOx formation to decrease. The CA50 and the peak pressure rise rate are shown in Figure 9. The CA50 is used as an indicator for the initial injection timing at 0% EGR. This value, as mentioned previously, is 9 ± 1 CAD ATDC and is based on past experience of optimal efficiency for this test setup for engine speeds of 900 rpm and above. With increasing EGR, the ignition delay tends to increase as the thermal and dilution effects of EGR reduces the reactivity during ignition stage. Consequently, the CA50 gets retarded for all engine speeds. For the low speed case, the initial CA50 is 12 CAD. Further advance of the CA50 by advancing the diesel injection timing is not possible for this speed since the peak pressure rise rate (Figure 9) exceeds the 15 bar/CAD hardware limit.

The peak pressure rise rate is an important hardware limitation for all engines. Excessively high pressure rise rate can cause driveability issues since it can lead to higher physical noise, vibration and harshness during the engine operation. Excessively high peak pressure rise rate can also cause physical damage to the engine. The peak pressure rise rate is especially an issue at lower engine speeds with extended cycle times since it reduces the ability to advance the injection timing. With increasing EGR, the CA50 is retarded and majority of the combustion occurs further away from the compression

TDC of the engine, which leads to lower peak pressure rise rates (Figure 9).

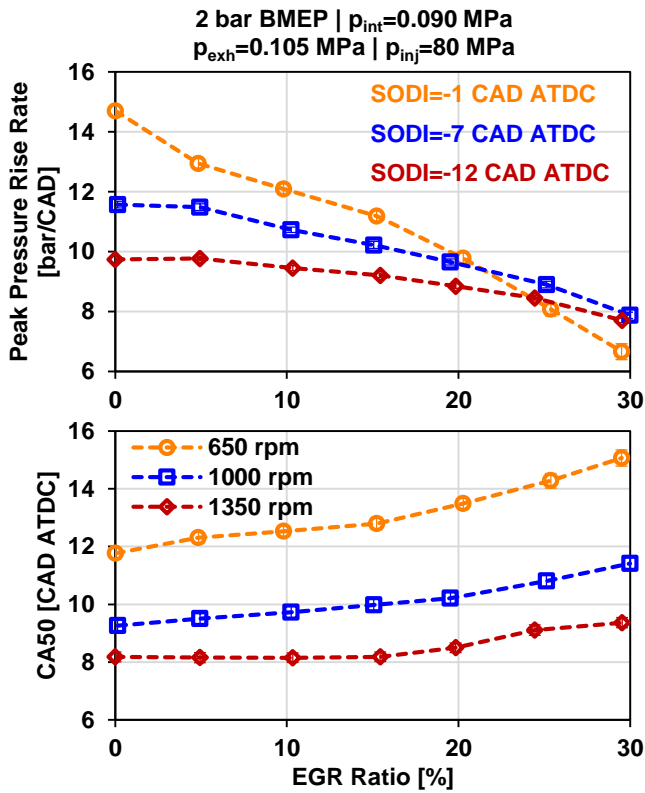


Figure 9. Effect of EGR on peak pressure rise rate (top) and CA50 (bottom)

Figure 10 shows the exhaust gas temperature profile, BTE and brake specific NOx emissions (denoted by bsNOx) for the given test cases. Exhaust gas temperatures decrease with decreasing engine speed. The cause can be the reduced number of combustion cycles per unit time as well as the lower heat generated by friction when the engine speed decreases. The exhaust gas temperature increases with increasing EGR at all engine speeds. Three factors may cause the variation of the exhaust temperature with increasing EGR. First, use of EGR can reduce the combustion temperatures since it increases the heat capacity of the in-cylinder charge, which tends to decrease the exhaust gas temperature. Second, the use of EGR increases the intake gas temperature (Figure 8), which may cause an increase in the exhaust gas temperature. Third, if the CA50 is retarded with the use of EGR, fuel combustion occurs later in the cycle and can cause the exhaust temperature to increase as well. A combination of these three factors may explain the variation in the exhaust gas temperature with increasing EGR. The CA50 retardation of 3 CAD for the low speed case is greater than the ~1.5 CAD retardation of the medium and high speed cases, which may cause the greater change in exhaust gas temperature for the low speed case in comparison to the exhaust gas temperature change of the medium and high speed cases. Exhaust gas temperatures in the steady state tests are above 200 °C for all engine speeds and therefore, a close-coupled SCR unit can be deployed.

The BTE decreases for the low speed case as the EGR is increased. This may be due to the retarded CA50 which causes a decrease in combustion efficiency. For the medium speed case, the BTE does not show significant change over the EGR sweep, since the CA50 is within the range of 8-11 CAD ATDC. The BTE is the maximum for the medium speed case compared to those of low and high speed cases. Page 9 of 13

For the high speed case, the BTE improves marginally. This might be due to further optimization of the CA50 when the EGR rate is increased.

The NOx emissions decrease with increasing EGR as expected since the thermal, dilution, and chemical effects of EGR tend to inhibit NOx formation. The increase in NOx emissions with decreasing engine speed can be attributed to the increase in NOx formation in the post flame region, since the lower the engine speed, the longer the post flame duration. With 30% EGR, the engine-out bsNOx can be reduced to ~2 g/kWh for all engine speed cases. Current emission standard of 0.2 g/bhp-hr (~0.27 g/kWh) is achievable with a close-coupled SCR unit with a conversion efficiency of ~80-90%. However, achieving ultra-low NOx of ~0.02 g/bhp-hr would be difficult under these experimental conditions with this test setup. Further strategies to reduce the engine-out NOx emissions while maintaining the exhaust temperature have to be investigated.

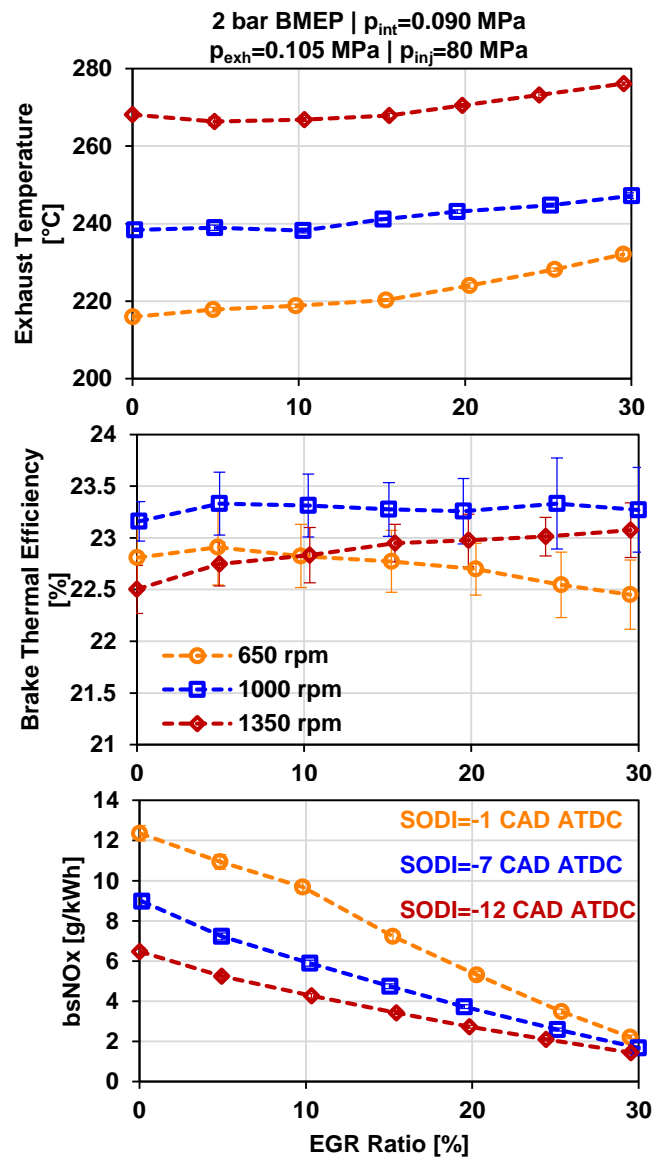


Figure 10. Effect of EGR on exhaust temperature (top), brake thermal efficiency (middle) and bsNOx (bottom)

Laboratory Test – Effect of Double Injection

One conclusion from the EGR sweep test is that given the exhaust gas temperature profile and the NO_x emissions, achieving ultra-low NO_x levels is difficult even with a close-coupled SCR catalyst. Therefore, the use of a double diesel injection is explored as means to further reduce the engine-out NO_x emissions and increase the exhaust gas temperature. The double diesel injection consists of a main injection event during the end of the compression stroke, and a post injection event during the expansion stroke. When the double injection is enabled with 30% EGR, the main injection timing has to be advanced to set the CA50 to 9±1 CAD ATDC. The post injection fuel quantity is 40% of the total fuel injection quantity. Based on the fuel injector map at 800 bar injection pressure, at 2 bar BMEP, 40% corresponds to the shortest possible injector opening command. The post injection timing is progressively retarded from 10 CAD ATDC to 30 CAD ATDC. The pressure and heat release traces are shown in Figure 11. The heat release rate of a double injection has a distinct second peak later in the expansion stroke corresponding to combustion of the post injection fuel. The peak cylinder pressures do not change significantly over the post injection timing sweep. There are distinct differences in the heat release rate. Expectedly, the second peak corresponding to the post injection is delayed as the post injection timing is retarded. The peak of the main heat release rate increases as well. This is probably due to decreasing combustion efficiency of the post injection fuel, which requires the main injection fuel quantity to be increased to maintain the load.

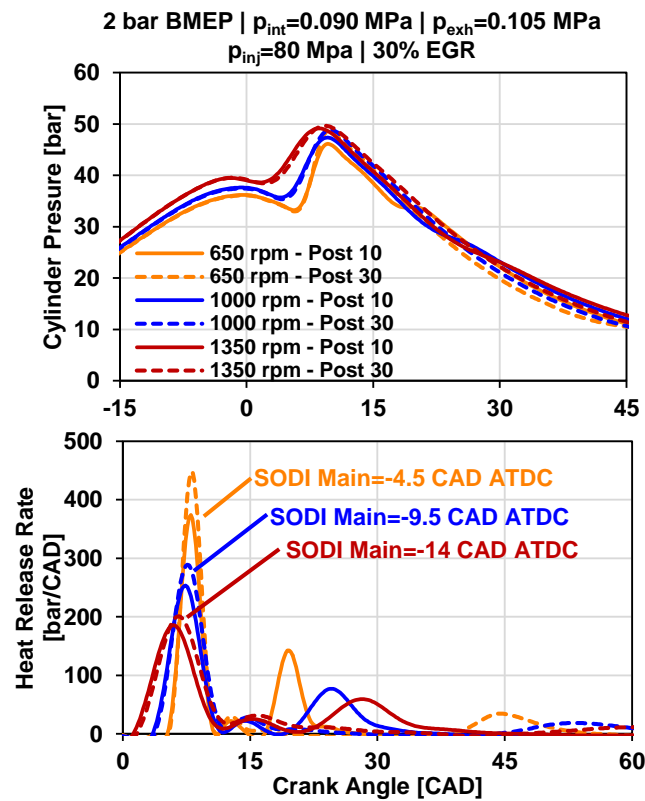


Figure 11. Effect of post injection timing on the cylinder pressure (top) and heat release rate (bottom)

The peak pressure rise rate and CA50 are shown in Figure 12. In general, the use of multiple injections distributes the energy release from the fuel over a longer duration of the engine cycle and thereby

causes a reduction in the peak pressure rise rate. While the pressure rise rate changes marginally for the medium and high speed cases, there is a more significant increase for the low speed case with retarding post injection timing. The increase in the main injection fuel quantity to compensate for the lower combustion efficiency of the post injection enhances the first heat release peak associated with pre-mixed combustion (Figure 11), which could have caused the peak pressure rise rate to be higher at a more retarded post injection timing, especially at low engine speeds when temporal duration of each engine cycle is longer.

The CA50 is advanced as the post injection timing is retarded. This is also caused by the increased injection duration of the main injection command to compensate for the lower combustion efficiency of the post injection fuel. The overall advance in the CA50 is less than 1 CAD for all engine speeds.

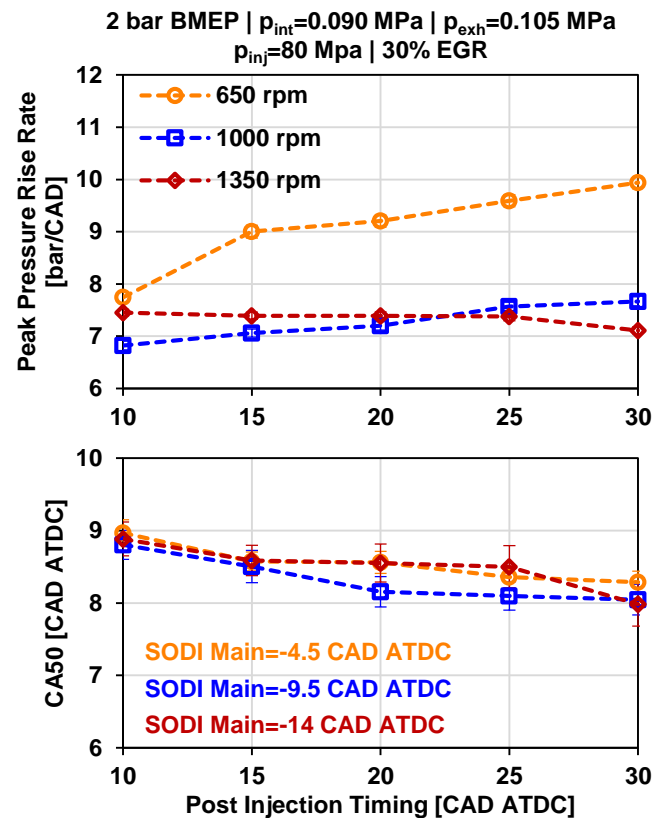


Figure 12. Effect of post injection timing on peak pressure rise rate (top) and CA50 (bottom)

The exhaust gas temperature, BTE and bsNO_x are shown in Figure 13. The corresponding data for single injection at 30% EGR are also shown on the figure for reference and marked by star symbols. The benefits of using the post injection to increase exhaust temperature and decrease NO_x emissions are more apparent for the medium and high engine speed cases. In general, retarding the post injection timing increases the exhaust gas temperature. This is probably due to the retardation of the second peak of heat release, which increases the gas temperatures later in the expansion stroke (Figure 11). At the low engine speed, owing to the longer time scale associated with each cycle, this heat energy can be lost through heat transfer to the walls of the combustion chamber. Hence, the change in exhaust gas

temperature over the post injection timing sweep is greater for the high engine speed case.

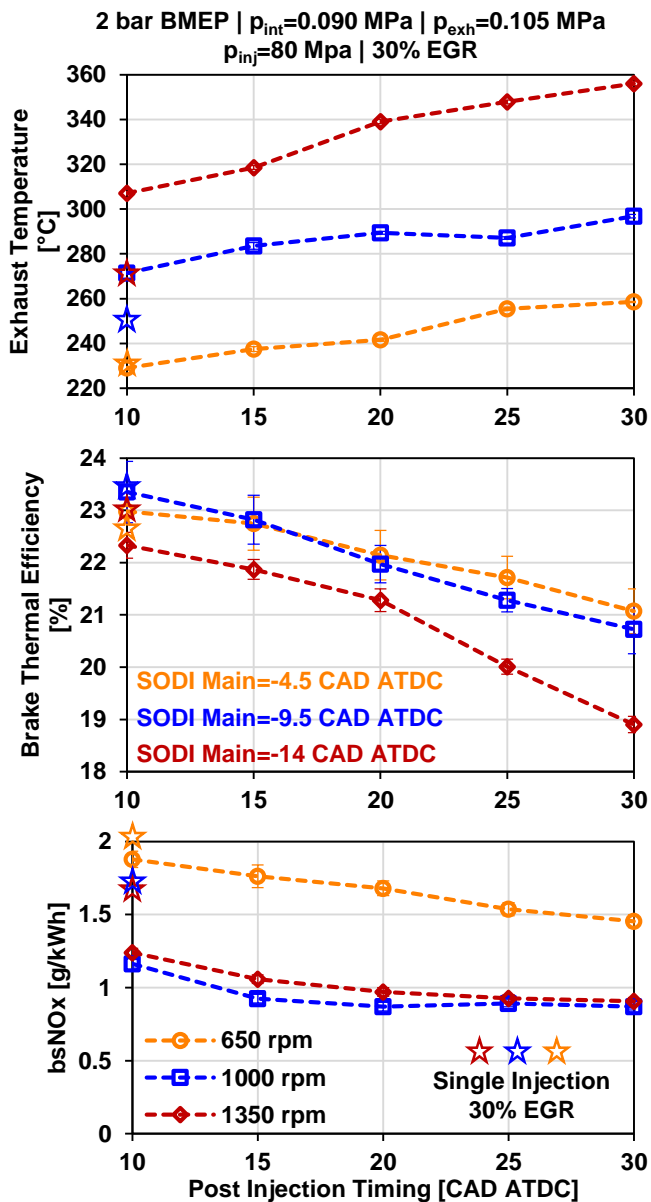


Figure 13. Effect of post injection timing on exhaust temperature (top), brake thermal efficiency (middle) and bsNOx (bottom)

Retarding the post-injection timing decreases the brake thermal efficiency due to under-utilization of the post-injection fuel as discussed previously. For the low speed case, when 30% EGR is used, the peak pressure rise rate is no longer a limiting factor for advancing the injection timing. With the combination of post injection, EGR, and optimized CA50, the BTE for low speed can be improved to 23% compared to 22.5%. The BTEs for low and medium engine speeds are similar since the losses associated with utilization of the post injection fuel associated with the medium engine speeds and heat transfer losses associated with the lower engine speeds may balance each other. At high speed, the adverse effect of post injection timing retard on BTE is most apparent since energy release from the post-injection fuel may be incomplete due to the short cycle duration.

The NOx emissions decrease with retarding post injection timing (Figure 13). A few factors can contribute to this. Through multiple injections and distributed energy release over a longer portion of the cycle, the temperatures associated with the combustion of the main diesel pulse decrease and therefore NOx formation rate reduces at the main combustion stage. The overall air-fuel ratio decreases due to lowered combustion efficiency in addition to the oxygen dilution effect of EGR. These two factors may minimize regions in the combustion chamber conducive to NOx formation in which temperatures are high and the air-fuel mixture is slightly lean. One reason why the post injection timing sweep was stopped at 30 CAD ATDC is the diminishing returns with respect to efficiency and no further reductions in NOx emissions. This implied that the post injection had limited participation in the in-cylinder combustion.

On-road testing data reported in literature indicates that there is a substantial challenge of achieving ultra-low NOx emissions in real-world applications since SCR temperatures can regularly drop below the urea injection activation threshold [16]. This implies that low temperature NOx control methods may have applications beyond cold start and idling conditions. Based on these results, it can be inferred that the medium engine speed (1000 rpm) with the use of 30% EGR and early post-injection can be a suitable compromise for minimizing engine-out NOx emissions and concurrently increasing the exhaust gas temperature and maintaining the BTE. There remain substantial challenges in improving the BTE of the engine at cold ambient temperatures. Additionally, since the engine is idling at a load (and not 0 bar BMEP in the strictest definition of idling), there is going to be an absolute increase in the fuel consumption. It is evident from DP-1 of the in-use testing that low load-low speed idling even over extended periods is insufficient to increase the exhaust gas temperature. Hence, as evidenced in literature and this study, there remain significant opportunities for optimization.

Conclusions

In-use test data confirms some of the observations reported in the literature especially with respect to the exhaust temperature and tail-pipe NOx emissions. The engine load is found to play a critical role at low exhaust temperatures since at higher loads, the engine-out NOx emissions would be higher, and these emissions would not be treated in the SCR if the exhaust gas temperatures are too low. In-use testing also shows that low load-low speed idling even over extended periods is insufficient to increase the exhaust gas temperature.

Based on the in-use test data, certain laboratory test parameters were adopted to provide research results relevant to practical applications. Preliminary thermal management strategies to increase exhaust gas temperature and reduce engine-out NOx emissions were evaluated by conducting steady state idle tests at different engine speeds at a constant low load. Using EGR was deemed to be a suitable strategy for decreasing engine-out NOx, pre-heating the intake charge into the engine and raising the exhaust gas temperature. The medium engine speed was found to be a reasonable compromise in terms of maintaining the brake thermal efficiency, reducing NOx emissions and maintaining sufficient exhaust temperature for thermal management. With 30% EGR as the baseline, use of double fuel injection (main injection + post injection) was investigated as means to further reduce NOx and increase exhaust temperature. Retarding the post injection timing may enhance the exhaust gas temperature, but there is a significantly adverse impact on efficiency especially at high engine speed. At low and medium engine speeds, with a post injection timing closer to the TDC, using a double injection could provide further reduction in NOx emissions over the 30% EGR baseline.

Future testing will focus on study of other engine operating parameters such as intake air pressure, injection pressure, and engine load on the NO_x emissions and exhaust temperature profile using cooled intake air. NO_x reduction in the SCR using DEF injection will also be evaluated in combination with engine-out NO_x reduction strategies.

References

- Government of Canada, Accessed from <https://www.canada.ca/en/environment-climate-change/services/environmental-indicators/air-pollutant-emissions.html#NOx>
- Environment and Climate Change Canada, "Canada's Air Pollutant Emissions Inventory Report: 1990-2018," Accessed from http://publications.gc.ca/collections/collection_2020/eccc/En81-30-2018-eng.pdf on November 15, 2020.
- Environment Protection Agency, USA, "EPA Acting Administrator Wheeler Launches Cleaner Trucks Initiative," Accessed from <https://www.epa.gov/newsreleases/epa-acting-administrator-wheeler-launches-cleaner-trucks-initiative> on December 3, 2018.
- Environment Protection Agency, USA, "Advance Notice of Proposed Rule: Control of Air Pollution from New Motor Vehicles: Heavy-Duty Engine Standards," Accessed from <https://www.epa.gov/regulations-emissions-vehicles-and-engines/advance-notice-proposed-rule-control-air-pollution-new> on January 15, 2020.
- California Air Resources Board, Accessed from <https://ww2.arb.ca.gov/our-work/programs/heavy-duty-low-nox/about> on October 30, 2018.
- Manufacturers of Emissions Controls Association, "Technology Feasibility for Heavy-Duty Diesel Trucks in Achieving 90% Lower NO_x Standards in 2027," Accessed from www.meca.org/resources/MECA_2027_Low_NOx_White_Paper_FINAL.pdf on March 01, 2020.
- Government of Canada, Accessed from <https://open.canada.ca/data/en/dataset/000fe5aa-1d77-42d1-bfe7-458c51dacfef> on April 10, 2020
- Christopher A. Sharp, Cynthia C. Webb, Gary D. Neely, and Ian Smith, "Evaluating Technologies and Methods to Lower Nitrogen Oxide Emissions from Heavy-Duty Vehicles," ARB Sponsored Study (Contract 13-312) Final Report. Accessed from <https://ww2.arb.ca.gov/sites/default/files/classic/research/apr/past/13-312.pdf> on November 15, 2020.
- Culbertson, D., Khair, M., Zhang, S., Tan, J., and Spooler, J., "The Study of Exhaust Heating to Improve SCR Cold Start Performance" SAE International Journal of Engines 8 (3): 1187–95, 2015. <https://doi.org/10.4271/2015-01-1027>.
- Kamasamudram, K., Currier, N., Szailer, T., and Yezerets, A., "Why Cu- and Fe-zeolite SCR Catalysts Behave Differently at Low Temperatures," SAE Technical Paper 2010-01-1182, 2010.
- Zheng, M., Reader, G. T. and Hawley, J. G., "Diesel engine exhaust gas recirculation—a review on advanced and novel concepts," Energy Conversion and Management, vol. 45, no. 6, pp. 883-900, 4/2004, 2004. [https://doi.org/10.1016/S0196-8904\(03\)00194-8](https://doi.org/10.1016/S0196-8904(03)00194-8).
- Zelenka, P., Aufinger, H., Reczek, W. and Cartellieri, W., "Cooled EGR - A Key Technology for Future Efficient HD Diesels," SAE Technical Paper 980190, 1998. <https://doi.org/10.4271/980190>.
- Hountalas, D.T., Mavropoulos, G.C., and Binder, K.B., "Effect of Exhaust Gas Recirculation (EGR) Temperature for Various EGR Rates on Heavy Duty DI Diesel Engine Performance and Emissions," Energy 33, no. 2: 272–83, 2008. <https://doi.org/10.1016/j.energy.2007.07.002>.
- Sakunthalai, R. A., Xu, H., Liu, D., Tian, J., Wyszynski, M., and Piaszyk, J., "Impact of Cold Ambient Conditions on Cold Start and Idle Emissions from Diesel Engines." SAE Technical Paper 2014-01-2715, 2014. <https://doi.org/10.4271/2014-01-2715>
- Bai, S., Han, J., Liu, M., Qin, , Wang, G., and Li, G-X "Experimental Investigation of Exhaust Thermal Management on NO_x Emissions of Heavy-Duty Diesel Engine under the World Harmonized Transient Cycle (WHTC)." Applied Thermal Engineering 142 (September): 421–32, 2018. <https://doi.org/10.1016/j.applthermaleng.2018.07.042>.
- Boriboonsomsin, K., Durbin, T., Scora,., Johnson, K., Sandez, D., Vu, A., Jiang, Y., et al. "Real-World Exhaust Temperature Profiles of on-Road Heavy-Duty Diesel Vehicles Equipped with Selective Catalytic Reduction." Science of The Total Environment 634 (September 2018): 909–21. <https://doi.org/10.1016/j.scitotenv.2018.03.362>.
- Sharp, C., Webb, C., Neely, G., Sarlashkar, J. et al., "Achieving Ultra Low NO_x Emissions Levels with a 2017 Heavy-Duty On-Highway TC Diesel Engine and an Advanced Technology Emissions System - NO_x Management Strategies," SAE Int. J. Engines 10(4) , 2017, <https://doi.org/10.4271/2017-01-0958>.
- Sharp, C., Webb, C., Yoon, S., Carter, M., and Henry, C., "Achieving Ultra Low NO_x Emissions Levels with a 2017 Heavy-Duty On-Highway TC Diesel Engine - Comparison of Advanced Technology Approaches," SAE International Journal of Engines 10 (4), 2017. <https://doi.org/10.4271/2017-01-0956>
- Neely, G. D., Sharp, C., and Rao, S., "CARB Low NO_x Stage 3 Program-Modified Engine Calibration and Hardware Evaluations," SAE Technical Paper 2020-01-0318, 2020. <https://doi.org/10.4271/2020-01-0318>
- Zavala, B., Sharp, C., Neely, G., and Rao, S. "CARB Low NO_x Stage 3 Program-Aftertreatment Evaluation and Down Selection," SAE Technical Paper 2020-01-1402, 2020. <https://doi.org/10.4271/2020-01-1402>
- Lavoie, G. A., Heywood, J. B., and Keck, J. C., "Experimental and Theoretical Study of Nitric Oxide Formation in Internal Combustion Engines." Combustion Science and Technology 1, no. 4 (February 1970): 313–26, 1970. <https://doi.org/10.1080/00102206908952211>.
- Khair, M. K., Jääskeläinen, H., "Emission Formation in Diesel Engines," Accessed from https://www.dieselnet.com/tech/diesel_emiform.php#nox on October 10, 2018.
- Guo, H., Liu, F., and Smallwood, G. J., "A Numerical Study on NO_x Formation in Laminar Counterflow CH₄/Air Triple Flames." Combustion and Flame 143, no. 3 (November 2005): 282–98, 2005. <https://doi.org/10.1016/j.combustflame.2005.06.004>.
- Heywood, J.B., "Internal Combustion Engine Fundamentals," New York, McGraw-Hill, 1988.
- Selim, Mohamed Y. E. "Pressure–time characteristics in diesel engine fueled with natural gas." Renewable energy 22.4 (2001): 473-489, 2001. [https://doi.org/10.1016/S0960-1481\(00\)00115-4](https://doi.org/10.1016/S0960-1481(00)00115-4)

Contact Information

Shouvik Dev
 Low Carbon Fuels and Clean Combustion
 Energy, Mining and Environment
 National Research Council of Canada, Ottawa, Ontario, Canada
 Email: shouvik.dev@nrc-cnrc.gc.ca

Acknowledgments

This work was funded by Environment and Climate Change Canada and Transport Canada's ecoTECHNOLOGY for Vehicles (eTV) program. The support of National Research Council of Canada through the internal Advanced Clean Energy program is also acknowledged.

Definitions/Abbreviations

ASC	ammonia slip catalyst
ATDC	after top dead center
bs	brake specific
BMEP	brake mean effective pressure
BTDC	before top dead center
BTE	brake thermal efficiency
ccSCR	close-coupled selective catalytic reduction
CAD	crank angle degree
CO	carbon monoxide
CO₂	carbon dioxide
COV	coefficient of variation
CTI	Cleaner Trucks Initiative
DEF	diesel exhaust fluid
DI	direct injection
EAT	exhaust after-treatment
ECCC	Environment and Climate Change Canada
EGR	exhaust gas recirculation
EPA	Environmental Protection Agency
FTP	Federal Test Protocol (US EPA emission test cycle)
g/bhp-hr	grams per brakehorse power-hour
g/kWh	grams per kilowatt-hour
GVWR	gross vehicle weight rating
HC	hydrocarbon
HDV	heavy-duty vehicle (Canada on-road vehicle that has GVWR >8500 lb)

IMEP	indicated mean effective pressure
kg/h	kilograms per hour
kPa	kilopascal
MPa	megapascal
NO_x	nitrogen oxides (NO and NO ₂)
PM	particulate matter
PPRR	peak pressure rise rate
rpm	revolutions per minute
SCR	selective catalytic reduction
SCRE	single cylinder research engine
SODI	start of diesel injection
TC	Transport Canada
ULSD	ultra-low sulphur diesel
US	United States
VE	volumetric efficiency